Electronic Supplementary Information

Biomolecular environment, quantification, and intracellular localization of multifunctional magnetic SERS nanoprobes

Tina Büchner, Daniela Drescher, Virginia Merk, Heike Traub, Peter Guttmann, Stephan Werner, Gerd Schneider, Norbert Jakubowski, Janina Kneipp

Content

1.) ICP-MS parameters

Table S1: NWR213 operating parameters.

Wavelength / nm	213
Laser ablation method	Line scanning
He carrier gas flow rate/ L min^{-1}	1.0
Laser warm up / s	30
Wash out / s	10
Spot size / µm	15
Scan rate / µm s^{-1}	15
Repetition rate / Hz	10
Fluence / J cm^{-2} (adjusted laser energy / %)	0.3 (36 %)
Line distance / µm	10

Table S2: Element XR operating parameters used for LA coupling.

RF power / W	1350
Guard electrode	Platinum, active
Ar cooling gas flow rate / L min^{-1}	16
Ar auxiliary gas flow rate / L min^{-1}	0.95 - 1.10
Ar sample gas flow rate / L min^{-1}	0.60 - 0.62
Sample and skimmer cone	Ni
Mass resolution	Low (R = 300)
Scan optimization	Speed
Isotopes monitored	For Ag-Magnetite: $^{106}Pd^{++}$, ^{56}Fe, ^{57}Fe, ^{106}Pd, ^{107}Ag, ^{109}Ag; For Au-Magnetite: $^{106}Pd^{++}$, ^{56}Fe, ^{57}Fe, ^{196}Pt, ^{197}Au
Magnet settling time / s	0.1, 0.001, 0.001, 0.01, 0.001, 0.001
Runs x pass	175 - 220 (depending on the length of the line) x 1
Detection mode	All isotopes with SEM (triple)
Sample time / s	0.002
Samples per peak	100
Segment duration per isotope / s	0.01
Mass window per isotope / %	5
Search window / %	0
Integration window / %	5
Scan type	E-scan

Table S3: iCAP Qc ICP-MS operating parameters used for the analysis of digested composite particles and cell pellets.

Sample introduction system	Peltier-cooled cyclonic spray chamber (quartz glass) with MicroFlow PFA-ST nebulizer (100 µL min^{-1})
RF power / W	1550
Ar cooling gas flow rate / L min^{-1}	14
Ar auxiliary gas flow rate / L min^{-1}	0.65
Ar nebulizer flow rate / L min^{-1}	1.1
Sample and skimmer cone	Ni (high matrix skimmer insert)
Operation mode	KED
Cell gas He / mL min^{-1}	4.9
Dwell time / ms	10
Main runs	10
Sweeps	10
Isotopes monitored	^{56}Fe, ^{57}Fe, ^{107}Ag, ^{109}Ag, ^{197}Au

2.) UV-vis absorbance spectra and TEM images of composite structures

Since the nanostructures are used in experiments with cultured cells, their absorbance spectra were acquired in the presence of cell culture medium. After particle preparation, the spectrum of the Ag-Magnetite nanostructures shows a broad plasmon band with a maximum at 418 nm, indicative of individual silver nanoparticles that form nanoaggregates within the composite structures (**Fig. S1A**, dashed line) in agreement with the TEM data (**Fig. 1A, Fig. S1C-F**). For the case of Au-Magnetite (**Fig. S1B,** dashed line), the maximum is observed around 534 nm. Neither of the two spectra indicates further aggregation of the plasmonic nanoparticles upon addition of cell culture medium. In the case of Au-Magnetite (**Fig. S1B**, black line), an increase in the scattering contribution from the magnetite nanostructures is observed, with a slight red-shift of the plasmon band.

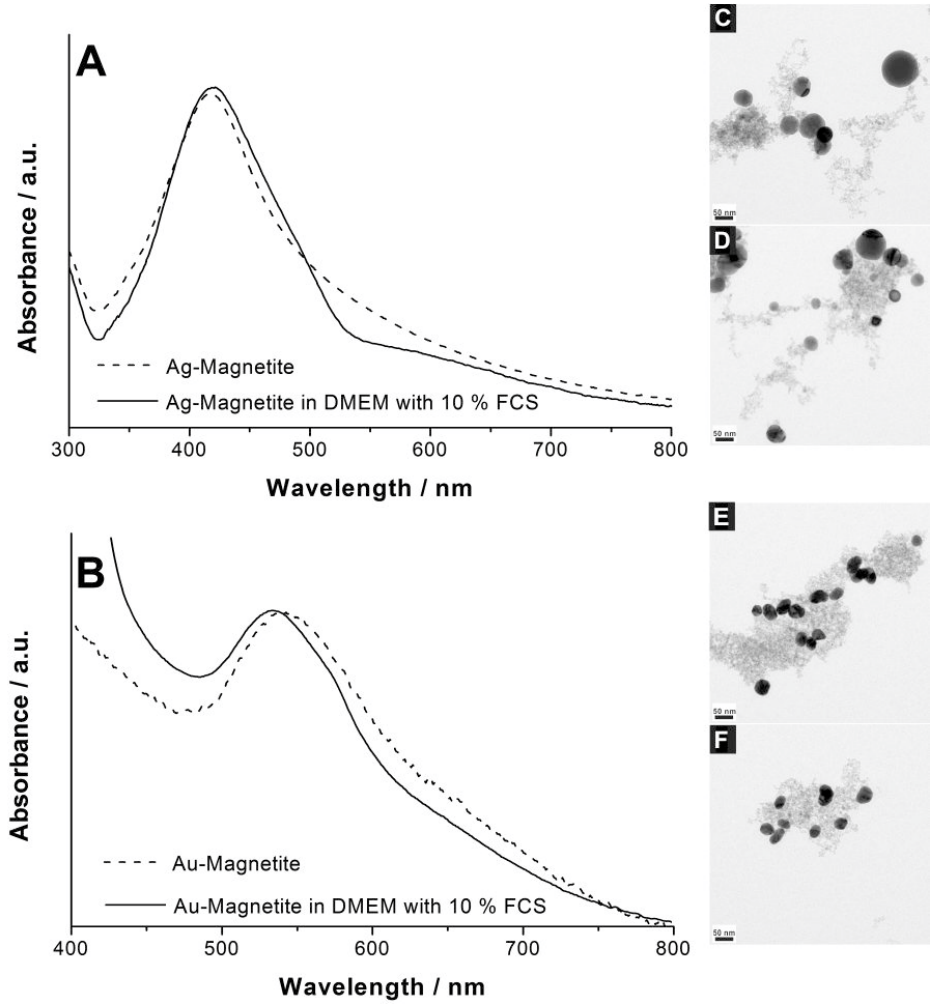

Fig. S1: Absorbance spectra of (**A**) Ag-Magnetite and (**B**) Au-Magnetite suspended in water (dashed line) and in cell culture medium (DMEM with 10 % FCS, black line) and their corresponding TEM images (Ag-Magnetite: **C, D**; Au-Magnetite: **E, F**), respectively. Scale bars: 50 nm

3.) Toxicity of composite structures

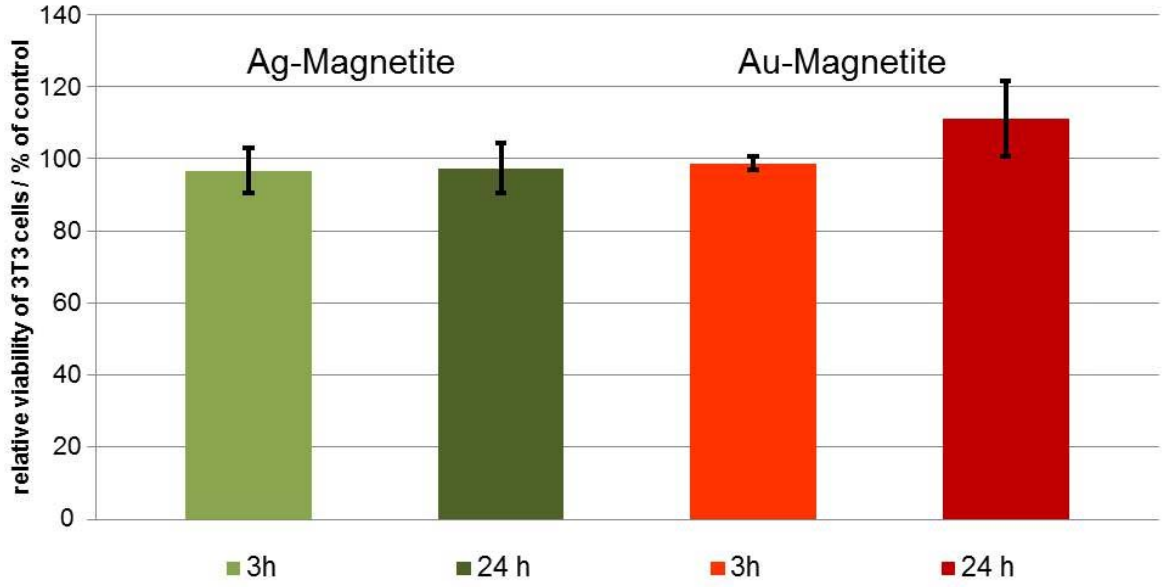

Fig. S2: Viability of 3T3 cells after 3 hours and 24 hours exposure to Ag-Magnetite (green bars) and Au-Magnetite (red bars) in culture medium, respectively, as determined by XTT assay.

4.) Band assignments of the SERS signals

Tab. S4: Tentative band assignments of SERS signals according to ref.[1-7]. Abbreviations: Tyr, tyrosine; Cys, cysteine; Pro, proline; Trp, tryptophane; Leu, leucine; Phe, phenylalanine; sym, symmetric; asym; asymmetric; stretch, stretching; breathe, breathing; rock, rocking; wag, wagging, scissor, scissoring.

Raman shift (cm^{-1})	**tentative assignment**
360	protein skeletal deformation
400	Tyr: ring breathe
471	S-S-stretch, Cys/Pro: skeletal
500	S-S-stretch
629	Cys: C-S stretch
655	Cys: C-S stretch or Tyr side chain
715	amino acids deformation (COO^-)
770	Trp: Indol sym. breathe, Cys; Leu, Phe: COOH deformation
791	amino acid: NH_3^+ rock
830	Tyr: sym. ring breathe
920	Pro: ring stretch (C-C)
960	proteins: C-C stretch
1008	Phe: aromatic ring breathe
1047	in-plane ring deformation (CH)
1072	rock(NH_2), stretch(C-N)
1104	protein: C-N stretch
1135	Tyr: C-C stretch
1180	Thr: CH_3 rock, Tyr, Phe: ring vibration
1208	DMEM
1235	Trp: ring
1272	Proteins, lipids: Amide III, (CH_2/CH_3) deformation
1344	Proteins: CH_2, CH_3 wag, : CH_2 scissor, amino acids: CH_3 deformation
1448	lipids, proteins: deformation(CH_2, CH_3)
1547	proteins: Amide II, N-H deformation
1565	proteins: NH_3^+ asym deformation

5.) SERS imaging

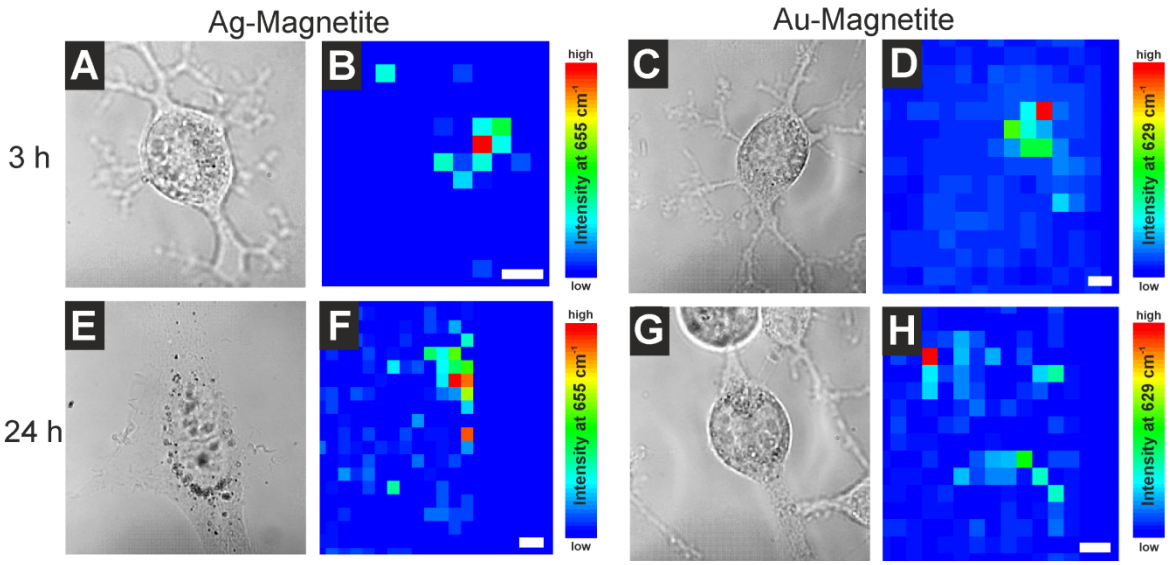

Fig. S3: SERS chemical maps and corresponding bright field images of 3T3 fibroblast cells incubated with Ag-Magnetite for 3 h (**A, B**) and 24 h (**E, F**) as well as with Au-Magnetite for 3 h (**C, D**) and 24 h (**G, H**). The relative intensity of the SERS signal at 655 cm^{-1} (ν(C−S) of cysteine) (**B, F**) and 629 cm^{-1} (ν(C−S) of cysteine) (**D, H**) are displayed. Scale bars: 4 µm. Excitation wavelength: 785 nm, accumulation time per spectrum: 1 s, intensity: 1.9 $\times 10^5$ Wcm^{-2}, step width: 2 µm.

6.) Distribution of nanoaggregate sizes of composite nanoparticles

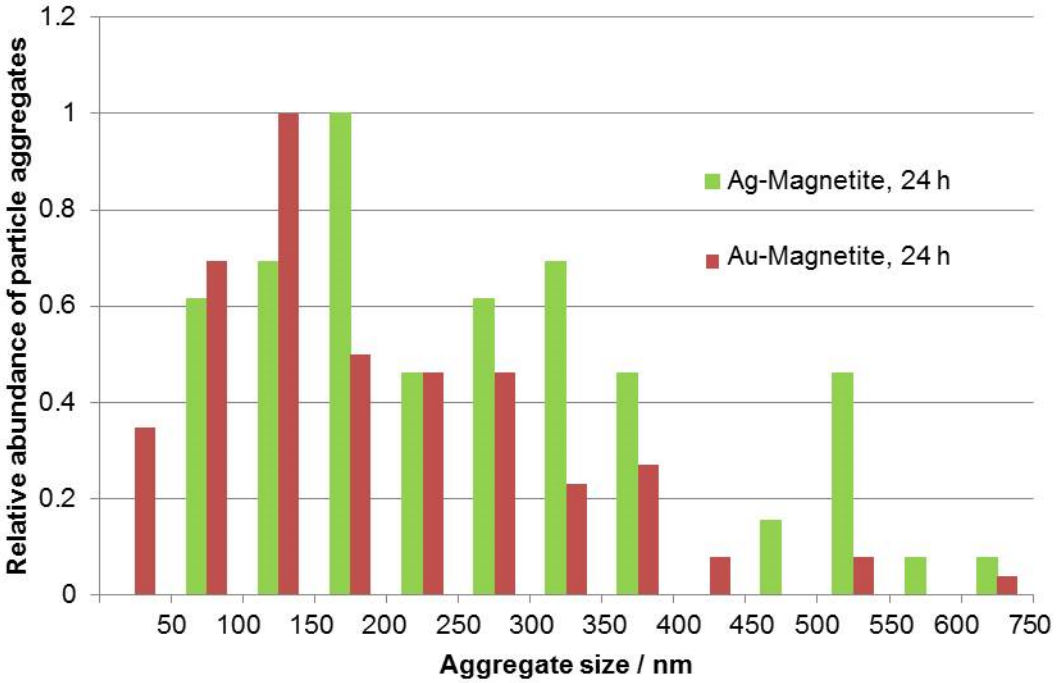

Fig. S4: Relative abundance of particle aggregates as function of nanoaggregate sizes of Ag-Magnetite (green bars) and Au-Magnetite (red bars) nanostructures inside 3T3 fibroblast cells after 24h-exposure. Aggregate sizes were determined by 3D X-ray microscopic imaging. The values are normalized to the maximum.

7.) References

1. F. S. Parker, *Applications of Infrared, Raman, and Resonance Raman Spectroscopy in Biochemistry*, Plenum Press New York, 1983.
2. G. Diaz Fleming, J. J. Finnerty, M. Campos-Vallette, F. Célis, A. E. Aliaga, C. Fredes and R. Koch, *J. Raman Spectrosc.*, 2009, 40, 632-638.
3. E. Podstawka, Y. Ozaki and L. M. Proniewicz, *Appl. Spectrosc.*, 2005, 59, 1516-1526.
4. S. Stewart and P. M. Fredericks, *Spectrochim. Acta Part A Mol. Biomol. Spectrosc.*, 1999, 55, 1641-1660.
5. J. De Gelder, K. De Gussem, P. Vandenabeele and L. Moens, *J. Raman Spectrosc.*, 2007, 38, 1133-1147.
6. D. Drescher, P. Guttmann, T. Büchner, S. Werner, G. Laube, A. Hornemann, B. Tarek, G. Schneider and J. Kneipp, *Nanoscale*, 2013, 5, 9193-9198.
7. D. Drescher, I. Zeise, H. Traub, P. Guttmann, S. Seifert, T. Büchner, N. Jakubowski, G. Schneider and J. Kneipp, *Adv. Funct. Mater.*, 2014, 24, 3765-3775.